

Solar-Mass Primordial Black Holes Explain NANOGrav Hint of Gravitational Waves

Kazunori Kohri^{a,b,c} and Takahiro Terada^d

^a *Institute of Particle and Nuclear Studies, KEK, 1-1 Oho, Tsukuba, Ibaraki 305-0801, Japan*

^b *The Graduate University for Advanced Studies (SOKENDAI),
1-1 Oho, Tsukuba, Ibaraki 305-0801, Japan*

^c *Kavli Institute for the Physics and Mathematics of the Universe (WPI),
University of Tokyo, Kashiwa 277-8583, Japan*

^d *Center for Theoretical Physics of the Universe,
Institute for Basic Science (IBS), Daejeon, 34126, Korea*

Abstract

The NANOGrav collaboration for the pulsar timing array (PTA) observation recently announced evidence of an isotropic stochastic process, which may be the first detection of the stochastic gravitational-wave (GW) background. We discuss the possibility that the signal is caused by the second-order GWs associated with the formation of solar-mass primordial black holes (PBHs). This possibility can be tested by future interferometer-type GW observations targeting the stochastic GWs from merger events of solar-mass PBHs as well as by updates of PTA observations.

1 Introduction

Gravitational-wave (GW) astronomy started with the successful observations of GWs from merger events of binary black holes by LIGO/Virgo collaborations [1]. GWs are also a valuable probe for the early Universe cosmology and particle physics. In particular, interests in primordial black holes (PBHs) [2–4] were reactivated after the first detection of GWs [5–7]. In the PBH scenario, GWs can be emitted not only from the merger of binary PBHs but also from the enhanced curvature perturbations that form PBHs [8–10]. This is due to the scalar-tensor mode couplings appearing at the second-order of the cosmological perturbation theory [11–16]. It is interesting that we can indirectly probe physics of inflation by probing the primordial scalar (curvature/density) perturbations inferred from the second-order GWs and PBH abundances [17–23].

Recently, the North American Nanohertz Observatory for Gravitational Waves (NANOGrav) released its 12.5-year pulsar timing array (PTA) data [24]. They search for an isotropic stochastic GW background by analyzing the cross-power spectrum of pulsar timing residuals. They reported evidence of a stochastic process, parametrized as a power-law, whose amplitude and slope are common among pulsars. The significance of the quadrupole nature in the overlap reduction function is not conclusive, whereas the monopole and dipole are relatively disfavored. This implies that the NANOGrav collaboration might have detected an astrophysical or cosmological stochastic GW background.

It should be noted that the NANOGrav 12.5-yr signal strength is greater than the upper bound derived in their previous 11-yr result [25] as well as that in Parkes PTA (PPTA) [26] (see Ref. [27] for the NANOGrav 11-yr constraints on PBHs and also Ref. [28] related particularly to European PTA (EPTA) constraints [29]). This apparent tension is explained primarily by the different choices of the Bayesian priors [24, 30], so all analyses can be correct given their assumptions including the priors. Specifically, the most relevant prior is on the amplitude of the red noise component associated with each pulsar. Previous PTA analyses used the uniform prior in the linear scale, whereas the NANOGrav 12.5-yr analyses used the uniform prior in the log scale. The effect of the difference is studied in detail in Ref. [30], and they found that the injected GW signal in their simulations tends to be absorbed by the red noise component more easily in the case of the (linearly) uniform prior. Moreover, the 95% confidence-level upper bound on the amplitude of the GW becomes smaller than the injected GW signal in about 50% of their simulations. This implies that the previous analyses are conservative for GW detection, but it can be regarded as aggressive in terms of upper limits. In this way, the putative GW signal and existing constraints can be consistent with each other once we take into account the differences of the priors on the pulsar red

noise. To claim the detection of the GW signals, however, it is also crucial to establish the quadrupole (Hellings-Downs [31]) nature of the GWs.

Assuming the observed stochastic process is due to the detection of stochastic GW background, the NANOGrav paper [24] studied the possibility that the GWs are produced from supermassive black hole merger events (e.g., see Ref. [32]). Other possibilities for the sources of GWs include cosmic strings [33–35], the PBH formation [36, 37], and a phase transition of a dark (hidden) sector [38, 39].

In this paper, we discuss the possibility that the putative GW signal is the second-order GWs induced by the curvature perturbations that produced solar-mass PBHs. The main difference from Refs. [36, 37] is the mass range of the dominant PBH component. Ref. [36] concluded that the solar-mass PBHs abundance must be negligible and also that the supermassive black holes may be responsible for the NANOGrav signal. Ref. [37] considered a wide spectrum of the curvature perturbations and studied the possibility that the dark matter abundance is explained by $\mathcal{O}(10^{-14})$ solar mass PBHs and a subdominant abundance of the solar-mass PBHs explain the NANOGrav signal. Further comparisons with Refs. [36, 37] are made in Section 5. We compare the second-order GWs and the NANOGrav result in Section 2 and interpret it in terms of PBH parameters in Section 3. Then, we discuss future tests of the scenario by measuring the stochastic GW background from mergers of solar-mass PBHs in Section 4. After the discussion in Section 5, we conclude in Section 6. We adopt the natural unit $\hbar = c = 8\pi G = 1$.

2 NANOGrav signals and second-order GWs

NANOGrav measures the strain of the GWs which is assumed to be of the power-law type in the relevant range of the analysis,

$$h(f) = A_{\text{GWB}} \left(\frac{f}{f_{\text{yr}}} \right)^\alpha, \quad (1)$$

where f is the frequency, $f_{\text{yr}} = 3.1 \times 10^{-8}$ Hz, A_{GWB} is the amplitude, and α is the slope. More directly, they measure the timing-residual cross-power spectral density, whose slope is parametrized as $-\gamma = 2\alpha - 3$. They report preferred ranges of the parameter space spanned by A_{GWB} and γ .

These parameters are related to the energy-density fraction parameter $\Omega_{\text{GW}}(f) = \rho_{\text{GW}}(f)/\rho_{\text{total}}$ in the following way, where ρ_{total} is the total energy density of the Universe and the GW

energy density is given by $\rho_{\text{GW}} = \int d \ln f \rho_{\text{GW}}(f)$: [25]

$$\Omega_{\text{GW}}(f) = \frac{2\pi^2 f_{\text{yr}}^2}{3H_0^2} A_{\text{GWB}}^2 \left(\frac{f}{f_{\text{yr}}} \right)^{5-\gamma}, \quad (2)$$

where $H_0 \equiv 100h \text{ km/s/Mpc}$ is the current Hubble parameter.

In this paper, we discuss the possibility to explain the putative signal by the secondary, curvature-induced GWs produced at the formation of $\mathcal{O}(1)M_{\odot}$ PBHs. For such PBHs, it turns out that $f \gtrsim f_{\text{yr}}$ does not contribute significantly, and so we consider the frequency range $2.5 \times 10^{-9} \text{ Hz} \leq f \leq 1.2 \times 10^{-8} \text{ Hz}$ [24, 33], which corresponds to the orange contour of figure 1 of Ref. [24].

The current strength of the second-order, curvature-induced GWs is given by $\Omega_{\text{GW}}(f) = D\Omega_{\text{GW},c}(f)$, where $D = (g_*(T)/g_{*,0})(g_{*,s,0}/g_{*,s}(T))^{4/3}\Omega_r$ is the dilution factor after the matter-radiation equality time with Ω_r being the radiation fraction¹, and $\Omega_{\text{GW},c}(f)$ is the asymptotic value of $\Omega_{\text{GW}}(f)$ well after the production of the GWs but before the equality time. This is given by

$$\Omega_{\text{GW},c}(f) = \frac{1}{12} \left(\frac{2\pi f}{aH} \right)^2 \int_0^{\infty} dt \int_{-1}^1 ds \left[\frac{t(t+2)(s^2-1)}{(t+s+1)(t-s+1)} \right]^2 \times \overline{I^2(t, s, k\eta_c)} \mathcal{P}_{\zeta}(\pi(t+s+1)f) \mathcal{P}_{\zeta}(\pi(t-s+1)f), \quad (3)$$

where aH is the conformal Hubble parameter evaluated at the conformal time η_c , $\mathcal{P}_{\zeta}(k)$ is the dimensionless power spectrum of the primordial curvature perturbations, and $\overline{I^2(t, s, k\eta_c)}$ is the oscillation average of the kernel function, whose analytic formula has been derived in Refs. [41, 42]. For the recent discussions on gauge (in)dependence, see Refs. [43–51].

For the primordial curvature perturbations, we assume that there is a smooth local peak on top of the quasi-scale-invariant power spectrum measured at the cosmic-microwave-background (CMB) scale. Such a peak can be approximated by the log-normal power spectrum

$$\mathcal{P}_{\zeta}(k) = \frac{A_s}{\sqrt{2\pi\sigma^2}} \exp\left(-\frac{(\ln k/k_*)^2}{2\sigma^2}\right), \quad (4)$$

where $k = 2\pi f$ is the wave number, A_s is the amplitude, σ^2 is the variance, and $\ln k_*$ is

¹For simplicity, we assume the Standard Model degrees of freedom and that neutrinos are massless. $g_*(T)$ and $g_{*,s}(T)$ are the effective relativistic degrees of freedom for the energy density and the entropy density, respectively [40]. These are evaluated at the horizon entry of the corresponding mode, while the quantities with the subscript 0 are evaluated at the present time.

the average. (One can match the position of the peak, its height, and its width by the Taylor series expansion. Note that the tail parts do not need to be precisely approximated as the log-normal function.) We take $\sigma = 1$ throughout the paper as a simple representative value. An $\mathcal{O}(1)$ value of σ can be expected, e.g., if one assumes that the local feature of $\mathcal{P}_\zeta(k)$ originates from a local feature of the inflaton potential, which can be, e.g., a locally flat part (an approximate inflection point) [52], a bump, or a dip [53] in the single-field case, corresponding to some physical phenomenon occurring in $\mathcal{O}(1)$ e-folding time of the Hubble expansion.² We treat A_s and k_* as free parameters. These can be translated to the GW parameters A_{GWB} and γ and to the PBH parameters f_{PBH} and M_{PBH} , which are defined below. In the case of the log-normal power spectrum, the full (approximate) analytic formula of $\Omega_{\text{GW},c}(f)$ is available [58] although we compute it numerically with the aid of extrapolation into the IR tail using the formula of Ref. [60].

An example of the spectrum of the second-order GWs is shown as the thick black line in Fig. 1. Also shown are power-law lines whose amplitude and slope correspond to points on the contours of the NANOGrav favored region on the (A_{GWB}, γ) -plane (the green contours in Fig. 2). The blue and cyan lines correspond to points on the upper half of 1σ and 2σ contours, while the orange and yellow lines correspond to points on the lower half of 1σ and 2σ contours, respectively. The shaded regions are the constraints from the previous PTA observations: EPTA [29], NANOGrav 11-yr [25], and PPTA [26]. The pink line at the bottom right is the prospective constraint of SKA [61].

In the figure, there seems an apparent tension between the NANOGrav 12.5-yr result and the existing PTA constraints. As mentioned in the introduction, this does not necessarily mean contradiction, but it reflects the intrinsic uncertainties of Bayesian analyses. The uniform prior on the red noise for each pulsar (adopted in the existing constraints) tends to pre-assign and overestimate the power in red noise components [30], and the reweighting of the samples of the previous data in accordance with the log-uniform prior indeed weaken the previous constraints [24, 30]. An ongoing joint investigation among the PTA datasets implies a similar tendency to the results of Ref. [24] also for data other than those of NANOGrav 11-yr [24] (namely, EPTA and PPTA). Therefore, we do not worry too much about the apparent tension between these preexisting PTA constraints and our explanation for the NANOGrav 12.5-yr hint of the GWs in the following analyses.

²There are many models that produce such a locally enhanced peak of $\mathcal{P}_\zeta(k)$. For constructions in the supergravity or string(-inspired) models, see, e.g., Refs. [54–57] and references therein. Also, the effects of changing σ on the second-order GWs and on PBHs are studied, e.g., in Ref. [58] and Ref. [59], respectively.

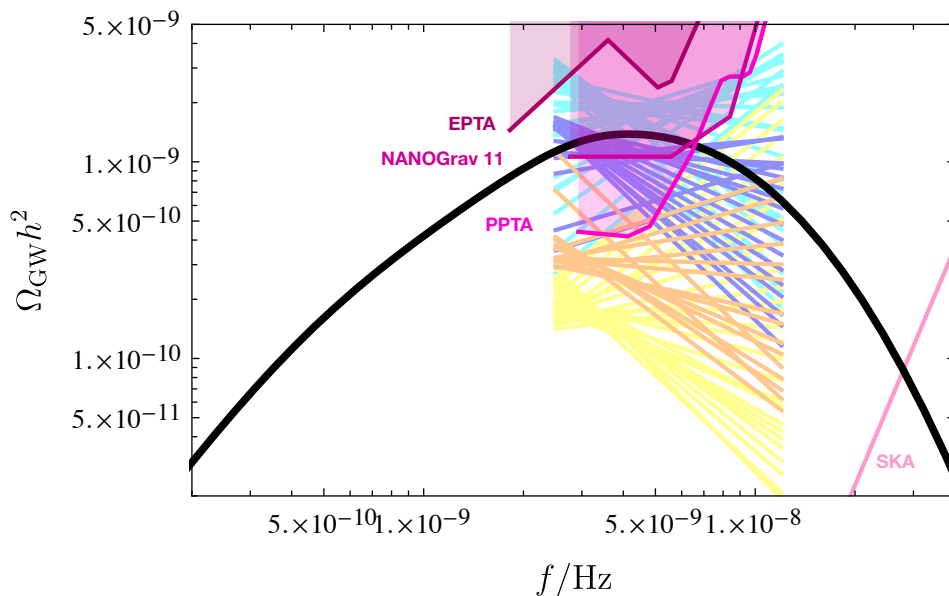


Figure 1: Example of the spectrum of the second-order GWs induced by the curvature perturbations that produced PBHs of $M_{\text{PBH}} = 1M_{\odot}$ and $f_{\text{PBH}} = 1 \times 10^{-4}$ (thick black line). The power-law lines in the interval $2.5 \times 10^{-9} \text{ Hz} \leq f \leq 1.2 \times 10^{-8} \text{ Hz}$ are also shown that correspond to a rough visual guide of the NANOGrav signal range. The amplitudes and slopes of blue (cyan) and orange (yellow) lines are on the upper and lower 1σ (2σ) contours of the NANOGrav signal, respectively. The previous PTA constraints are shown by shaded regions: EPTA [29], NANOGrav 11-yr [25], and PPTA [26]. The pink line at the bottom right is the prospective constraint of SKA [61].

3 Implications for the PBH mass and its abundance

The relations between the second-order GWs and the properties of PBHs are as follows. The GWs are induced by the enhanced curvature perturbations, which also produce PBHs. The energy density fraction β of the PBHs at the formation time, which also has the meaning of the formation probability of a PBH in a given Hubble patch, is calculated in the Press-Schechter formalism [62]³ as

$$\beta = \int_{\delta_c}^{\infty} d\delta \frac{1}{\sqrt{2\pi\sigma_2^2}} \exp\left(-\frac{\delta^2}{2\sigma_2^2}\right) \simeq \frac{1}{2} \text{Erfc}\left(\frac{\delta_c}{\sqrt{2\sigma_2^2}}\right), \quad (5)$$

where we have assumed that the primordial curvature perturbations have the Gaussian statistics, δ_c is the critical value of the coarse-grained density perturbations that produces

³For simplicity, we adopt the Press-Schechter formalism in this paper. However, we would like the readers to refer to Refs. [63–67] for more rigorous treatments.

a PBH [68–74], for which we take $\delta_c = 0.42$ [74, 75]⁴, Erfc is the complementary error function, and the variance σ_2^2 of the coarse-grained density perturbations is defined as

$$\sigma_2^2(k) = \frac{16}{81} \int_{-\infty}^{\infty} d \ln x w^2(x) x^4 \mathcal{P}_\zeta(xk), \quad (6)$$

where $w(x)$ is the window function, which we take as the modified Gaussian function $w(x) = \exp(-x^2/4)$. This window function was introduced in Ref. [76] and used as one of the two benchmark choices for the window function in Ref. [59]. Note that the choice of the window function significantly affects the abundance of the PBHs [77] (see also Ref. [78]) unless compensating parameters for the critical collapse are taken [59]. We will come back to this point in the discussion section.

The present energy density fraction of PBHs relative to cold dark matter is denoted by $f_{\text{PBH}} = \rho_{\text{PBH}}/\rho_{\text{CDM}}$. This is related to β as follows,

$$f_{\text{PBH}} = \int d \ln M \frac{\Omega_m}{\Omega_{\text{CDM}}} \frac{g_*(T)}{g_*(T_{\text{eq}})} \frac{g_{*,s}(T_{\text{eq}})}{g_{*,s}(T)} \frac{T}{T_{\text{eq}}} \epsilon \beta, \quad (7)$$

where the subscript m and eq denote the non-relativistic matter and the equality time, the temperature T is evaluated at the horizon entry of the corresponding mode k , and ϵ denotes the fraction of the horizon mass that goes into the PBH, which we take $\epsilon = 3^{-3/2}$ [4]. More detailed explanation for PBH formation and parameter dependencies can be found, e.g., in Refs. [79, 80] and in reviews [81–86].

We relate k and the horizon mass in the standard way, i.e., using the Friedmann equation. Note, however, that there is a discrepancy between the average PBH mass M_{PBH} and a naive horizon mass corresponding to k_* because of two reasons: the peak position of $\sigma_2^2(k)$ is smaller than k_* , and each PBH mass is ϵ times smaller than the corresponding horizon mass. These shifts of peak positions were discussed, e.g., in Ref. [87] and recently emphasized again [59].

Concretely, the relation among the wave number k_* , the corresponding frequency $f_* = k_*/(2\pi)$, the corresponding horizon mass M , and the average PBH mass M_{PBH} is as follows:

$$\frac{M_{\text{PBH}}}{1.0 M_\odot} \simeq \frac{M}{0.31 M_\odot} \simeq \left(\frac{k_*}{3.3 \times 10^6 \text{ Mpc}^{-1}} \right)^{-2} \simeq \left(\frac{f_*}{5.0 \times 10^{-9} \text{ Hz}} \right)^{-2}. \quad (8)$$

⁴ For the modified Gaussian window function, it is stated that $\delta_c = 0.18$ in Table 1 of Ref. [76] without a detailed derivation. This may apparently be at odds with a naive expectation that δ_c should be higher than in the case of other window functions for the window-function dependence to be suppressed since the modified Gaussian window function enhances the value of σ_2^2 . For this reason, we take $\delta_c = 0.42$ as the value used more frequently in the literature.

We vary the scalar amplitude in the range $0.015 \leq A_s \leq 0.040$ and the average PBH mass in the range $0.2 \leq M_{\text{PBH}}/M_\odot \leq 5$. The resultant $\Omega_{\text{GWB}}h^2$ is fitted by a power-law line in the aforementioned range $2.5 \times 10^{-9} \text{ Hz} \leq f \leq 1.2 \times 10^{-8} \text{ Hz}$ to extract the amplitude of the GW strain A_{GWB} and the slope γ . Note that $A_{\text{GWB}} \propto A_s$, but it also depends on k_* (or M_{PBH}) since the pivot scale is fixed to f_{yr} (see eq. (1)). The result is shown in Fig. 2. From the figure, we see that a large fraction of the scanned parameter space can explain the NANOGrav signal.

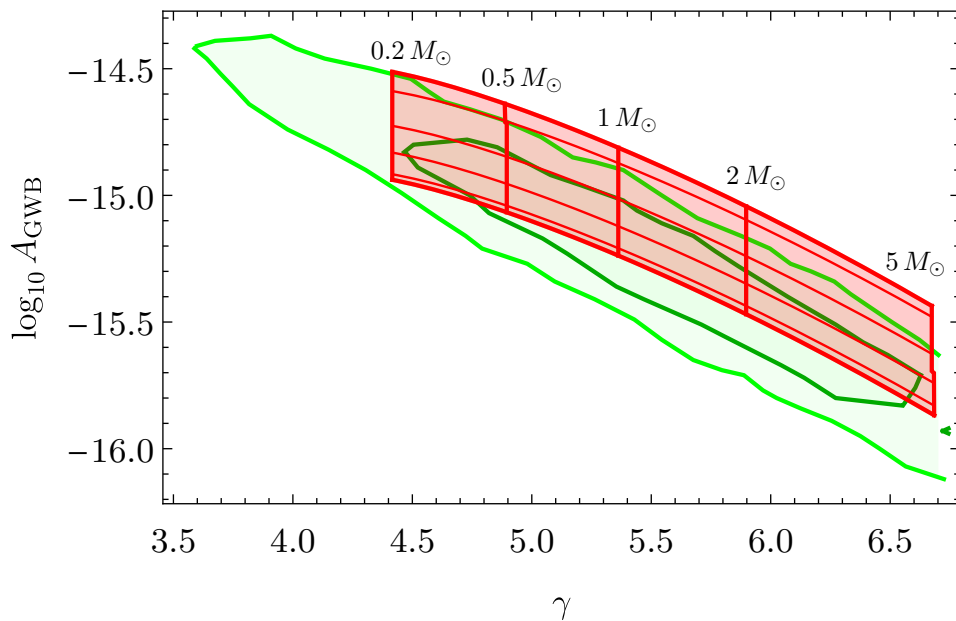


Figure 2: Parameter scan in the range $0.015 \leq A_s \leq 0.040$ and $0.2 \leq M_{\text{PBH}}/M_\odot \leq 5$ shown as the red shaded region. A larger A_s corresponds to a larger A_{GWB} , and a larger M_{PBH} corresponds to a larger γ . The thin red lines correspond to $f_{\text{PBH}} = 10^{-1}$, 10^{-4} , 10^{-7} , and 10^{-10} from top to bottom. The 1σ and 2σ NANOGrav contours are also shown.

The scanned parameter range for A_s corresponds to that of the PBH abundance f_{PBH} as shown in Fig. 3. The upper and lower ends correspond to $M_{\text{PBH}} = 0.2M_\odot$ and $5M_\odot$, respectively.

Combining the information in Figs. 2 and 3, one can map the NANOGrav contours onto the PBH parameter space $(M_{\text{PBH}}, f_{\text{PBH}})$, which are shown as the green contours in Fig. 4. The non-smoothness of the contours largely originates from the non-smoothness of the original NANOGrav contours. The uncertainty of extracting the data from the original contours is magnified in this figure compared to Fig. 2. Therefore, the 1σ and 2σ boundary has an uncertainty of very roughly an order of magnitude.

Fig. 4 shows that the PBH mass should be around a solar mass to explain the NANOGrav

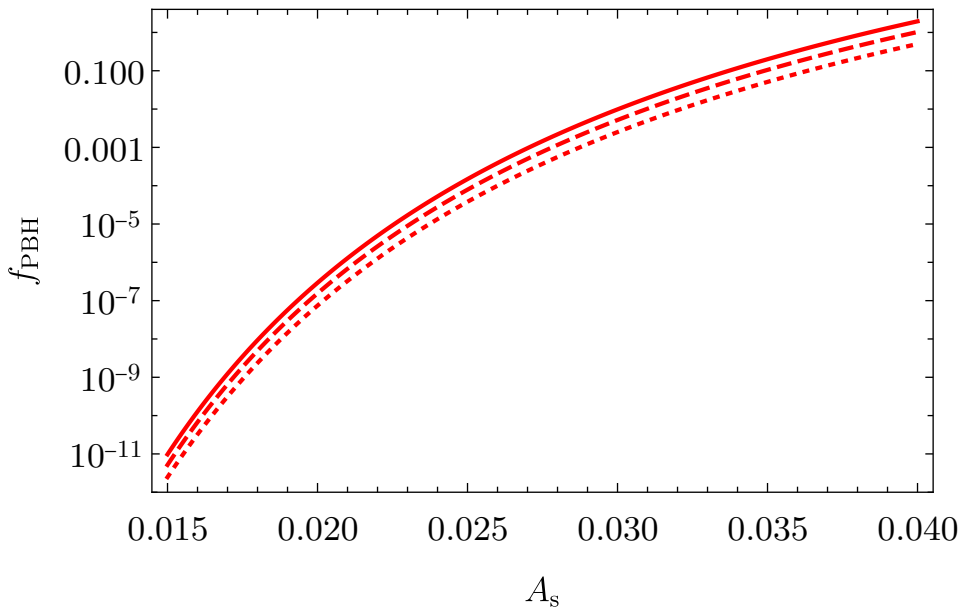


Figure 3: Relation between the scalar amplitude A_s and the PBH abundance f_{PBH} for $M_{\text{PBH}}/M_{\odot} = 0.2$ (top, solid), 1 (middle, dashed), and 5 (bottom, dotted).

signal. Also, it shows that f_{PBH} close to unity is disfavored, but $f_{\text{PBH}} \sim 0.1$ is within the 2σ contour depending on the value of M_{PBH} .

A part of such regions is excluded by existing constraints shown by shaded regions at the top of the figure. These include the microlensing constraints by EROS/MACHO collaborations [88, 89], the caustic crossing constraint [90], Advanced LIGO constraints on the subsolar mass range (individual events [91] and superposition of events [92, 93]), and the constraints due to photo-emission during gas accretion onto PBHs [94–96]. There are many subdominant but independent and complementary constraints around this mass range (see Ref. [85]). There is also the LIGO/Virgo constraints on supersolar mass range [97, 98]. Ref. [98] implies a substantial dependence on the width of the mass function, so we do not include it in Fig. 4.

4 Testing the scenario with the GWs from mergers

The solar-mass PBH possibility for NANOGrav can be tested by the detection of stochastic GW background from the superposition of binary solar-mass PBH merger events. The GW

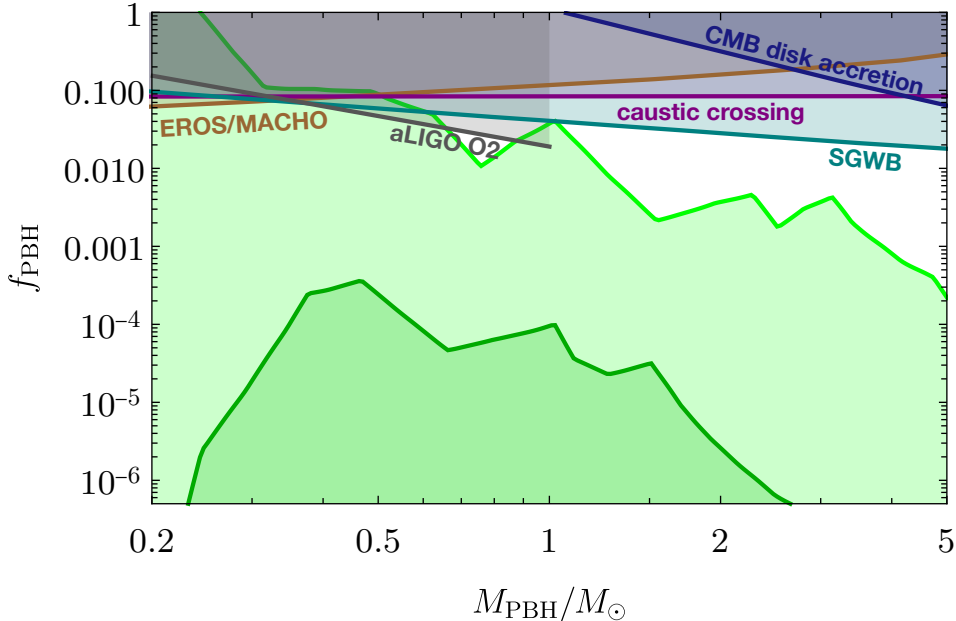


Figure 4: NANOGrav contours (green) on the plane of the average PBH mass M_{PBH} and the PBH abundance f_{PBH} . The dark shaded regions at the top are constraints from EROS-2 [88] and MACHO [89] (brown), caustic crossing [90] (purple), Advanced LIGO O2 (subsolar mass range) [91] (gray), Advanced LIGO non-detection of the stochastic GW background [92, 93] (cyan), and the E -mode polarization of the CMB due to the disk-shaped gas accretion [94] (blue).

spectrum is obtained as

$$\Omega_{\text{GW}}^{\text{merger}}(f) = \frac{f}{3H_0^2} \int_0^{\frac{f_{\text{cut}}}{f} - 1} dz \frac{R(z)}{(1+z)H(z)} \frac{dE_{\text{GW}}}{df_s}, \quad (9)$$

where $f_{\text{cut}} (= \mathcal{O}(1/M_{\text{PBH}}))$ is the UV cutoff frequency at the source frame (i.e., without the redshift factor) (see Refs. [99, 100] for the IR “cutoff” frequency), f_s is the frequency at the source frame, z is the redshift, R is the comoving merger rate, and E_{GW} is the energy of the GWs at the source frame. The expressions of f_{cut} , R , and dE_{GW}/df_s are found in Appendices B and C of Ref. [87]. See also Refs. [7, 84, 92, 101, 102] for more details. The frequency f_{cut} is just the maximal cutoff appearing around the end of the merger process.

The result is shown in Fig. 5 as the black lines where $M_{\text{PBH}} = 1M_{\odot}$ and $f_{\text{PBH}} = 10^{-2}$ (solid), 10^{-3} (dashed), 10^{-4} (dotted), and 10^{-5} (dot-dashed). Various prospective constraints (see the caption)⁵ as well as the lines in Fig. 1 are also shown. We do not show the M_{PBH}

⁵Though not shown in the figure, see also the following references for related experiments: ALIA [121], ELGAR [122], MAGIS [123, 124], MIGA [125], Taiji [126], and ZAIGA [127].

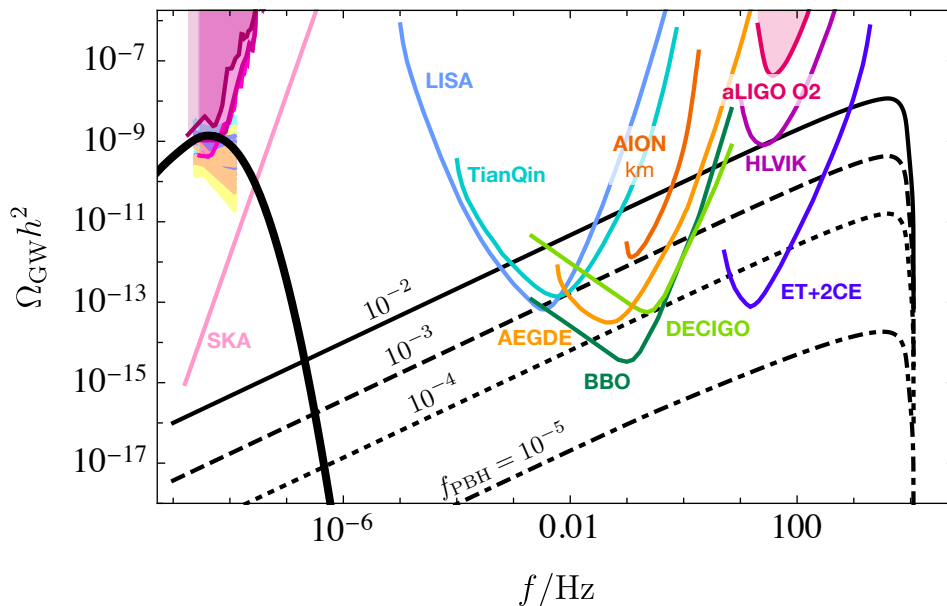


Figure 5: GW spectrum from the superposition of binary PBH merger events (thin black) with $M_{\text{PBH}} = 1M_{\odot}$ and $f_{\text{PBH}} = 10^{-2}$ (solid), 10^{-3} (dashed), 10^{-4} (dotted), and 10^{-5} (dot-dashed). Future prospects of various GW observations are also shown: SKA [61], LISA [103], TianQin [104, 105], BBO [106], DECIGO [107], AION [108], AEDGE [109], Advanced LIGO Hanford and Livingston [110] combined with Advanced Virgo [111] as well as LIGO India [112, 113] and KAGRA [114, 115] (HLVIK), and Einstein Telescope [116] and two third-generation Cosmic Explorers [117] (ET+2CE). The shaded red region is the Advanced LIGO O2 constraint [118]. Sensitivity curves have been read from Refs. [33, 108, 119, 120]. The top side of the figure is the upper bound $\Omega_{\text{GW}} h^2 < 1.8 \times 10^{-6}$ from the (non-)adiabatic N_{eff} bound of big-bang nucleosynthesis [42]. The existing PTA constraints and NANOGrav power-law guides are also shown as in Fig. 1.

dependence in the figure, but the spectra shift to the left as M_{PBH} increases. Eq. (8) clearly shows that the characteristic frequency f_* of the second-order GWs scales as $M_{\text{PBH}}^{-1/2}$, whereas the counterpart for the GWs from mergers scales as $f_{\text{cut}} \sim M_{\text{PBH}}^{-1}$ (see the text below eq. (9)) as demonstrated in Ref. [87]. Note that the thick black line corresponds to the second-order GWs for $M_{\text{PBH}} = 1M_{\odot}$ and $f_{\text{PBH}} = 10^{-4}$, but the f_{PBH} dependence is weak (see Fig. 3). The top end of the figure is the upper bound $\Omega_{\text{GW}} h^2 < 1.8 \times 10^{-6}$ [42] from the fact that the GWs contribute to the effective number of neutrinos N_{eff} and affect the big-bang nucleosynthesis. We can see from the figure that a large part of the parameter space can be probed by the future GW observations.

5 Discussion

Our results depend on various assumptions. Some of them have been already stated, but we emphasize them again. First, we do not consider the effect of the critical collapse [83, 128–130] since it occurs only when the spherical symmetry is precisely respected. It is clear that the rare high-peak has approximately the spherical shape [131], but the spherical symmetry must be realized to high precision for the critical collapse to happen [68]. On the other hand, Refs. [36, 37] include the effect of the critical collapse. It will be interesting to compare our results with an analysis including the critical collapse effect using a consistent parameter set [59]. In our preliminary study, we found a qualitatively similar feature that f_{PBH} tends to become larger than those reported in Refs. [36, 37].

Second, we have chosen the modified Gaussian window function, whose width is twice as large as the standard Gaussian window function. This boosts the value of f_{PBH} for a given value of A_s . This may be the largest difference compared to Refs. [36, 37] in which much smaller f_{PBH} 's were reported.

Third, we have not taken into account the nonlinear relation between the primordial curvature perturbations and the density perturbations (see Refs. [63, 132]). This inevitably leads to non-Gaussianity of the density perturbations [132]. Also, the inclusion of the intrinsic non-Gaussianity of the primordial curvature perturbations significantly affects f_{PBH} [23, 133, 134]. It also affects the second-order GWs [23, 135–139].

Fourth, we have not included the transfer function of the curvature perturbations in the definition of σ_2^2 . This is preferred in Ref. [76]. If we include the transfer function, however, σ_2^2 will reduce by “several” percent. This reduces f_{PBH} non-negligibly.

It is also worth mentioning that we have not taken into account the softening of the equation-of-state during the phase transition/crossover of quantum chromodynamics (QCD). See Refs. [37, 140, 141] for its enhancement effect on the PBH abundance f_{PBH} for a given scalar amplitude A_s . Depending on the boost factor, this may realize a better fit for the NANOGrav signal simultaneously with stronger and more easily detectable GWs from mergers of the solar-mass binary PBHs. The softening also slightly affects the spectrum of the second-order GWs [142].

We discussed a possible detection of the PBHs with the masses of $\mathcal{O}(1)M_\odot$ only by a future interferometer-type GW observations in Section 4. Complementarily, however, we can also measure such PBHs by the future optical/IR telescopes through microlensing events, e.g., Subaru HSC towards M31 for 10 year observations [143] or by the future precise CMB observations of E - and B -mode polarization due to photon emission from an accretion disk around a PBH, e.g., by LiteBIRD [144] or CMB-S4 [145].

6 Conclusion

In this paper, we have interpreted the recently reported NANOGrav 12.5-yr excess of the timing-residual cross-power spectral density in the low-frequency part as a stochastic GW background. We conclude that, under our assumptions, the second-order GWs induced by the curvature perturbations that produced a substantial amount of $\mathcal{O}(1)$ solar-mass PBHs can explain the NANOGrav stochastic GW signal. In particular, the abundance of the PBHs can be sufficiently large so that future GW observations can test this possibility by measuring the stochastic GW background produced by mergers of the solar-mass PBHs. This is nontrivial since the suitable scalar amplitude A_s could a priori produce too many PBHs that are excluded by existing observational constraints or too few PBHs that do not lead to the detectable stochastic GW background from merger events. Similarly, for a given f_{PBH} , the second-order GWs could be too strong or weak. Since the relation between A_s and f_{PBH} depends crucially on the ambiguity for the choice of the windows function as discussed in the previous section, a further study to refine the PBH formation criterion is necessary.

Note Added

Taking into account the uncertainties of PBH abundance calculations, i.e., the different choices of the window function, the value of δ_c (see footnote 4), etc., our results are largely consistent with those of Ref. [37] [146]. The difference from Ref. [36] is also discussed in the note added in Ref. [36]. In our paper, we do not claim that $\mathcal{O}(30)M_\odot$ PBHs responsible for the LIGO/Virgo events can explain the NANOGrav signal.

Acknowledgments

K.K. thanks Misao Sasaki and Shi Pi for useful discussions. We thank Valerio De Luca, Gabriele Franciolini, and Antonio Riotto for useful discussions. This work was supported by JSPS KAKENHI Grant Number JP17H01131 (K.K.), MEXT KAKENHI Grant Numbers JP19H05114 (K.K.) and JP20H04750 (K.K.), and IBS under the project code, IBS-R018-D1 (T.T.).

References

- [1] **LIGO Scientific, Virgo** Collaboration, B. Abbott *et al.*, “GWTC-1: A Gravitational-Wave Transient Catalog of Compact Binary Mergers Observed by LIGO and

- Virgo during the First and Second Observing Runs,” *Phys. Rev. X* **9** no. 3, (2019) 031040, [arXiv:1811.12907 \[astro-ph.HE\]](#).
- [2] S. Hawking, “Gravitationally collapsed objects of very low mass,” *Mon. Not. Roy. Astron. Soc.* **152** (1971) 75.
- [3] B. J. Carr and S. Hawking, “Black holes in the early Universe,” *Mon. Not. Roy. Astron. Soc.* **168** (1974) 399–415.
- [4] B. J. Carr, “The Primordial black hole mass spectrum,” *Astrophys. J.* **201** (1975) 1–19.
- [5] S. Bird, I. Cholis, J. B. Muñoz, Y. Ali-Haïmoud, M. Kamionkowski, E. D. Kovetz, A. Raccanelli, and A. G. Riess, “Did LIGO detect dark matter?,” *Phys. Rev. Lett.* **116** no. 20, (2016) 201301, [arXiv:1603.00464 \[astro-ph.CO\]](#).
- [6] S. Clesse and J. García-Bellido, “The clustering of massive Primordial Black Holes as Dark Matter: measuring their mass distribution with Advanced LIGO,” *Phys. Dark Univ.* **15** (2017) 142–147, [arXiv:1603.05234 \[astro-ph.CO\]](#).
- [7] M. Sasaki, T. Suyama, T. Tanaka, and S. Yokoyama, “Primordial Black Hole Scenario for the Gravitational-Wave Event GW150914,” *Phys. Rev. Lett.* **117** no. 6, (2016) 061101, [arXiv:1603.08338 \[astro-ph.CO\]](#). [Erratum: *Phys.Rev.Lett.* 121, 059901 (2018)].
- [8] R. Saito and J. Yokoyama, “Gravitational wave background as a probe of the primordial black hole abundance,” *Phys. Rev. Lett.* **102** (2009) 161101, [arXiv:0812.4339 \[astro-ph\]](#). [Erratum: *Phys.Rev.Lett.* 107, 069901 (2011)].
- [9] R. Saito and J. Yokoyama, “Gravitational-Wave Constraints on the Abundance of Primordial Black Holes,” *Prog. Theor. Phys.* **123** (2010) 867–886, [arXiv:0912.5317 \[astro-ph.CO\]](#). [Erratum: *Prog.Theor.Phys.* 126, 351–352 (2011)].
- [10] E. Bugaev and P. Klimai, “Induced gravitational wave background and primordial black holes,” *Phys. Rev.* **D81** (2010) 023517, [arXiv:0908.0664 \[astro-ph.CO\]](#).
- [11] K. Tomita, “Non-linear theory of gravitational instability in the expanding universe,” *Progress of Theoretical Physics* **37** no. 5, (1967) 831–846.
- [12] S. Matarrese, O. Pantano, and D. Saez, “General relativistic dynamics of irrotational dust: Cosmological implications,” *Phys. Rev. Lett.* **72** (1994) 320–323, [arXiv:astro-ph/9310036 \[astro-ph\]](#).
- [13] S. Matarrese, S. Mollerach, and M. Bruni, “Second order perturbations of the Einstein-de Sitter universe,” *Phys. Rev.* **D58** (1998) 043504, [arXiv:astro-ph/9707278 \[astro-ph\]](#).

- [14] K. N. Ananda, C. Clarkson, and D. Wands, “The Cosmological gravitational wave background from primordial density perturbations,” *Phys. Rev.* **D75** (2007) 123518, [arXiv:gr-qc/0612013 \[gr-qc\]](#).
- [15] D. Baumann, P. J. Steinhardt, K. Takahashi, and K. Ichiki, “Gravitational Wave Spectrum Induced by Primordial Scalar Perturbations,” *Phys. Rev.* **D76** (2007) 084019, [arXiv:hep-th/0703290 \[hep-th\]](#).
- [16] H. Assadullahi and D. Wands, “Gravitational waves from an early matter era,” *Phys. Rev.* **D79** (2009) 083511, [arXiv:0901.0989 \[astro-ph.CO\]](#).
- [17] L. Alabidi, K. Kohri, M. Sasaki, and Y. Sendouda, “Observable Spectra of Induced Gravitational Waves from Inflation,” *JCAP* **09** (2012) 017, [arXiv:1203.4663 \[astro-ph.CO\]](#).
- [18] L. Alabidi, K. Kohri, M. Sasaki, and Y. Sendouda, “Observable induced gravitational waves from an early matter phase,” *JCAP* **05** (2013) 033, [arXiv:1303.4519 \[astro-ph.CO\]](#).
- [19] N. Orlofsky, A. Pierce, and J. D. Wells, “Inflationary theory and pulsar timing investigations of primordial black holes and gravitational waves,” *Phys. Rev. D* **95** no. 6, (2017) 063518, [arXiv:1612.05279 \[astro-ph.CO\]](#).
- [20] K. Inomata and T. Nakama, “Gravitational waves induced by scalar perturbations as probes of the small-scale primordial spectrum,” *Phys. Rev. D* **99** no. 4, (2019) 043511, [arXiv:1812.00674 \[astro-ph.CO\]](#).
- [21] C. T. Byrnes, P. S. Cole, and S. P. Patil, “Steepest growth of the power spectrum and primordial black holes,” *JCAP* **06** (2019) 028, [arXiv:1811.11158 \[astro-ph.CO\]](#).
- [22] I. Ben-Dayan, B. Keating, D. Leon, and I. Wolfson, “Constraints on scalar and tensor spectra from N_{eff} ,” *JCAP* **06** (2019) 007, [arXiv:1903.11843 \[astro-ph.CO\]](#).
- [23] C. Unal, E. D. Kovetz, and S. P. Patil, “Multi-messenger Probes of Inflationary Fluctuations and Primordial Black Holes,” [arXiv:2008.11184 \[astro-ph.CO\]](#).
- [24] **NANOGrav** Collaboration, Z. Arzoumanian *et al.*, “The NANOGrav 12.5-year Data Set: Search For An Isotropic Stochastic Gravitational-Wave Background,” [arXiv:2009.04496 \[astro-ph.HE\]](#).
- [25] **NANOGrav** Collaboration, Z. Arzoumanian *et al.*, “The NANOGrav 11-year Data Set: Pulsar-timing Constraints On The Stochastic Gravitational-wave Background,” *Astrophys. J.* **859** no. 1, (2018) 47, [arXiv:1801.02617 \[astro-ph.HE\]](#).

- [26] R. Shannon *et al.*, “Gravitational waves from binary supermassive black holes missing in pulsar observations,” *Science* **349** no. 6255, (2015) 1522–1525, [arXiv:1509.07320 \[astro-ph.CO\]](#).
- [27] Z.-C. Chen, C. Yuan, and Q.-G. Huang, “Pulsar Timing Array Constraints on Primordial Black Holes with NANOGrav 11-Year Data Set,” *Phys. Rev. Lett.* **124** no. 25, (2020) 251101, [arXiv:1910.12239 \[astro-ph.CO\]](#).
- [28] R.-G. Cai, S. Pi, S.-J. Wang, and X.-Y. Yang, “Pulsar Timing Array Constraints on the Induced Gravitational Waves,” *JCAP* **10** (2019) 059, [arXiv:1907.06372 \[astro-ph.CO\]](#).
- [29] L. Lentati *et al.*, “European Pulsar Timing Array Limits On An Isotropic Stochastic Gravitational-Wave Background,” *Mon. Not. Roy. Astron. Soc.* **453** no. 3, (2015) 2576–2598, [arXiv:1504.03692 \[astro-ph.CO\]](#).
- [30] J. S. Hazboun, J. Simon, X. Siemens, and J. D. Romano, “Model Dependence of Bayesian Gravitational-Wave Background Statistics for Pulsar Timing Arrays,” [arXiv:2009.05143 \[astro-ph.IM\]](#).
- [31] R. Hellings and G. Downs, “UPPER LIMITS ON THE ISOTROPIC GRAVITATIONAL RADIATION BACKGROUND FROM PULSAR TIMING ANALYSIS,” *Astrophys. J. Lett.* **265** (1983) L39–L42.
- [32] A. Sesana, F. Haardt, P. Madau, and M. Volonteri, “Low - frequency gravitational radiation from coalescing massive black hole binaries in hierarchical cosmologies,” *Astrophys. J.* **611** (2004) 623–632, [arXiv:astro-ph/0401543](#).
- [33] J. Ellis and M. Lewicki, “Cosmic String Interpretation of NANOGrav Pulsar Timing Data,” [arXiv:2009.06555 \[astro-ph.CO\]](#).
- [34] S. Blasi, V. Brdar, and K. Schmitz, “Has NANOGrav found first evidence for cosmic strings?,” [arXiv:2009.06607 \[astro-ph.CO\]](#).
- [35] W. Buchmuller, V. Domcke, and K. Schmitz, “From NANOGrav to LIGO with metastable cosmic strings,” [arXiv:2009.10649 \[astro-ph.CO\]](#).
- [36] V. Vaskonen and H. Veermäe, “Did NANOGrav see a signal from primordial black hole formation?,” [arXiv:2009.07832 \[astro-ph.CO\]](#).
- [37] V. De Luca, G. Franciolini, and A. Riotto, “NANOGrav Hints to Primordial Black Holes as Dark Matter,” [arXiv:2009.08268 \[astro-ph.CO\]](#).

- [38] Y. Nakai, M. Suzuki, F. Takahashi, and M. Yamada, “Gravitational Waves and Dark Radiation from Dark Phase Transition: Connecting NANOGrav Pulsar Timing Data and Hubble Tension,” [arXiv:2009.09754 \[astro-ph.CO\]](#).
- [39] A. Addazi, Y.-F. Cai, Q. Gan, A. Marciano, and K. Zeng, “NANOGrav results and Dark First Order Phase Transitions,” [arXiv:2009.10327 \[hep-ph\]](#).
- [40] K. Saikawa and S. Shirai, “Primordial gravitational waves, precisely: The role of thermodynamics in the Standard Model,” *JCAP* **05** (2018) 035, [arXiv:1803.01038 \[hep-ph\]](#).
- [41] J. R. Espinosa, D. Racco, and A. Riotto, “A Cosmological Signature of the SM Higgs Instability: Gravitational Waves,” *JCAP* **09** (2018) 012, [arXiv:1804.07732 \[hep-ph\]](#).
- [42] K. Kohri and T. Terada, “Semianalytic calculation of gravitational wave spectrum nonlinearly induced from primordial curvature perturbations,” *Phys. Rev. D* **97** no. 12, (2018) 123532, [arXiv:1804.08577 \[gr-qc\]](#).
- [43] J.-O. Gong, “Analytic integral solutions for induced gravitational waves,” [arXiv:1909.12708 \[gr-qc\]](#).
- [44] K. Tomikawa and T. Kobayashi, “Gauge dependence of gravitational waves generated at second order from scalar perturbations,” *Phys. Rev. D* **101** no. 8, (2020) 083529, [arXiv:1910.01880 \[gr-qc\]](#).
- [45] V. De Luca, G. Franciolini, A. Kehagias, and A. Riotto, “On the Gauge Invariance of Cosmological Gravitational Waves,” *JCAP* **03** (2020) 014, [arXiv:1911.09689 \[gr-qc\]](#).
- [46] K. Inomata and T. Terada, “Gauge Independence of Induced Gravitational Waves,” *Phys. Rev. D* **101** no. 2, (2020) 023523, [arXiv:1912.00785 \[gr-qc\]](#).
- [47] C. Yuan, Z.-C. Chen, and Q.-G. Huang, “Scalar induced gravitational waves in different gauges,” *Phys. Rev. D* **101** no. 6, (2020) 063018, [arXiv:1912.00885 \[astro-ph.CO\]](#).
- [48] M. Giovannini, “Spurious gauge-invariance of higher-order contributions to the spectral energy density of the relic gravitons,” *Int. J. Mod. Phys. A* **35** no. 27, (2020) 2050165, [arXiv:2005.04962 \[hep-th\]](#).
- [49] Y. Lu, A. Ali, Y. Gong, J. Lin, and F. Zhang, “On the gauge transformation of scalar induced gravitational waves,” [arXiv:2006.03450 \[gr-qc\]](#).
- [50] Z. Chang, S. Wang, and Q.-H. Zhu, “Gauge invariance of the second order cosmological perturbations,” [arXiv:2009.11025 \[astro-ph.CO\]](#).

- [51] A. Ali, Y. Gong, and Y. Lu, “Gauge transformation of scalar induced tensor perturbation during matter domination,” [arXiv:2009.11081 \[gr-qc\]](#).
- [52] J. M. Ezquiaga, J. Garcia-Bellido, and E. Ruiz Morales, “Primordial Black Hole production in Critical Higgs Inflation,” *Phys. Lett. B* **776** (2018) 345–349, [arXiv:1705.04861 \[astro-ph.CO\]](#).
- [53] S. S. Mishra and V. Sahni, “Primordial Black Holes from a tiny bump/dip in the Inflaton potential,” *JCAP* **04** (2020) 007, [arXiv:1911.00057 \[gr-qc\]](#).
- [54] K. Inomata, M. Kawasaki, K. Mukaida, and T. T. Yanagida, “Double inflation as a single origin of primordial black holes for all dark matter and LIGO observations,” *Phys. Rev. D* **97** no. 4, (2018) 043514, [arXiv:1711.06129 \[astro-ph.CO\]](#).
- [55] T.-J. Gao and Z.-K. Guo, “Primordial Black Hole Production in Inflationary Models of Supergravity with a Single Chiral Superfield,” *Phys. Rev. D* **98** no. 6, (2018) 063526, [arXiv:1806.09320 \[hep-ph\]](#).
- [56] M. Cicoli, V. A. Diaz, and F. G. Pedro, “Primordial Black Holes from String Inflation,” *JCAP* **06** (2018) 034, [arXiv:1803.02837 \[hep-th\]](#).
- [57] O. Özsoy, S. Parameswaran, G. Tasinato, and I. Zavala, “Mechanisms for Primordial Black Hole Production in String Theory,” *JCAP* **07** (2018) 005, [arXiv:1803.07626 \[hep-th\]](#).
- [58] S. Pi and M. Sasaki, “Gravitational Waves Induced by Scalar Perturbations with a Lognormal Peak,” [arXiv:2005.12306 \[gr-qc\]](#).
- [59] A. D. Gow, C. T. Byrnes, P. S. Cole, and S. Young, “The power spectrum on small scales: Robust constraints and comparing PBH methodologies,” [arXiv:2008.03289 \[astro-ph.CO\]](#).
- [60] C. Yuan, Z.-C. Chen, and Q.-G. Huang, “Log-dependent slope of scalar induced gravitational waves in the infrared regions,” *Phys. Rev. D* **101** no. 4, (2020) 043019, [arXiv:1910.09099 \[astro-ph.CO\]](#).
- [61] P. E. Dewdney, P. J. Hall, R. T. Schilizzi, and T. J. L. W. Lazio, “The square kilometre array,” *Proceedings of the IEEE* **97** no. 8, (Aug, 2009) 1482–1496.
- [62] W. H. Press and P. Schechter, “Formation of galaxies and clusters of galaxies by selfsimilar gravitational condensation,” *Astrophys. J.* **187** (1974) 425–438.
- [63] C.-M. Yoo, T. Harada, J. Garriga, and K. Kohri, “Primordial black hole abundance from random Gaussian curvature perturbations and a local density threshold,” *PTEP* **2018** no. 12, (2018) 123E01, [arXiv:1805.03946 \[astro-ph.CO\]](#).

- [64] T. Suyama and S. Yokoyama, “A novel formulation of the primordial black hole mass function,” *PTEP* **2020** no. 2, (2020) 023E03, [arXiv:1912.04687 \[astro-ph.CO\]](#).
- [65] C. Germani and R. K. Sheth, “Nonlinear statistics of primordial black holes from Gaussian curvature perturbations,” *Phys. Rev. D* **101** no. 6, (2020) 063520, [arXiv:1912.07072 \[astro-ph.CO\]](#).
- [66] A. Escrivà, C. Germani, and R. K. Sheth, “Analytical thresholds for black hole formation in general cosmological backgrounds,” [arXiv:2007.05564 \[gr-qc\]](#).
- [67] C.-M. Yoo, T. Harada, S. Hirano, and K. Kohri, “Abundance of Primordial Black Holes in Peak Theory for an Arbitrary Power Spectrum,” [arXiv:2008.02425 \[astro-ph.CO\]](#).
- [68] M. Shibata and M. Sasaki, “Black hole formation in the Friedmann universe: Formulation and computation in numerical relativity,” *Phys. Rev. D* **60** (1999) 084002, [arXiv:gr-qc/9905064](#).
- [69] I. Musco, J. C. Miller, and L. Rezzolla, “Computations of primordial black hole formation,” *Class. Quant. Grav.* **22** (2005) 1405–1424, [arXiv:gr-qc/0412063](#).
- [70] A. G. Polnarev and I. Musco, “Curvature profiles as initial conditions for primordial black hole formation,” *Class. Quant. Grav.* **24** (2007) 1405–1432, [arXiv:gr-qc/0605122](#).
- [71] I. Musco, J. C. Miller, and A. G. Polnarev, “Primordial black hole formation in the radiative era: Investigation of the critical nature of the collapse,” *Class. Quant. Grav.* **26** (2009) 235001, [arXiv:0811.1452 \[gr-qc\]](#).
- [72] I. Musco and J. C. Miller, “Primordial black hole formation in the early universe: critical behaviour and self-similarity,” *Class. Quant. Grav.* **30** (2013) 145009, [arXiv:1201.2379 \[gr-qc\]](#).
- [73] T. Nakama, T. Harada, A. Polnarev, and J. Yokoyama, “Identifying the most crucial parameters of the initial curvature profile for primordial black hole formation,” *JCAP* **01** (2014) 037, [arXiv:1310.3007 \[gr-qc\]](#).
- [74] T. Harada, C.-M. Yoo, and K. Kohri, “Threshold of primordial black hole formation,” *Phys. Rev. D* **88** no. 8, (2013) 084051, [arXiv:1309.4201 \[astro-ph.CO\]](#). [Erratum: *Phys.Rev.D* **89**, 029903 (2014)].
- [75] T. Harada, C.-M. Yoo, T. Nakama, and Y. Koga, “Cosmological long-wavelength solutions and primordial black hole formation,” *Phys. Rev. D* **91** no. 8, (2015) 084057, [arXiv:1503.03934 \[gr-qc\]](#).

- [76] S. Young, “The primordial black hole formation criterion re-examined: Parametrisation, timing and the choice of window function,” *Int. J. Mod. Phys. D* **29** no. 02, (2019) 2030002, [arXiv:1905.01230 \[astro-ph.CO\]](#).
- [77] K. Ando, K. Inomata, and M. Kawasaki, “Primordial black holes and uncertainties in the choice of the window function,” *Phys. Rev. D* **97** no. 10, (2018) 103528, [arXiv:1802.06393 \[astro-ph.CO\]](#).
- [78] K. Tokeshi, K. Inomata, and J. Yokoyama, “Window function dependence of the novel mass function of primordial black holes,” [arXiv:2005.07153 \[astro-ph.CO\]](#).
- [79] S. Young, C. T. Byrnes, and M. Sasaki, “Calculating the mass fraction of primordial black holes,” *JCAP* **07** (2014) 045, [arXiv:1405.7023 \[gr-qc\]](#).
- [80] K. Kohri and T. Terada, “Primordial Black Hole Dark Matter and LIGO/Virgo Merger Rate from Inflation with Running Spectral Indices: Formation in the Matter- and/or Radiation-Dominated Universe,” *Class. Quant. Grav.* **35** no. 23, (2018) 235017, [arXiv:1802.06785 \[astro-ph.CO\]](#).
- [81] M. Y. Khlopov, “Primordial Black Holes,” *Res. Astron. Astrophys.* **10** (2010) 495–528, [arXiv:0801.0116 \[astro-ph\]](#).
- [82] B. Carr, K. Kohri, Y. Sendouda, and J. Yokoyama, “New cosmological constraints on primordial black holes,” *Phys. Rev. D* **81** (2010) 104019, [arXiv:0912.5297 \[astro-ph.CO\]](#).
- [83] B. Carr, F. Kuhnel, and M. Sandstad, “Primordial Black Holes as Dark Matter,” *Phys. Rev. D* **94** no. 8, (2016) 083504, [arXiv:1607.06077 \[astro-ph.CO\]](#).
- [84] M. Sasaki, T. Suyama, T. Tanaka, and S. Yokoyama, “Primordial black holes—perspectives in gravitational wave astronomy,” *Class. Quant. Grav.* **35** no. 6, (2018) 063001, [arXiv:1801.05235 \[astro-ph.CO\]](#).
- [85] B. Carr, K. Kohri, Y. Sendouda, and J. Yokoyama, “Constraints on Primordial Black Holes,” [arXiv:2002.12778 \[astro-ph.CO\]](#).
- [86] B. Carr and F. Kuhnel, “Primordial Black Holes as Dark Matter: Recent Developments,” [arXiv:2006.02838 \[astro-ph.CO\]](#).
- [87] S. Wang, T. Terada, and K. Kohri, “Prospective constraints on the primordial black hole abundance from the stochastic gravitational-wave backgrounds produced by coalescing events and curvature perturbations,” *Phys. Rev. D* **99** no. 10, (2019) 103531, [arXiv:1903.05924 \[astro-ph.CO\]](#). [Erratum: *Phys.Rev.D* 101, 069901 (2020)].

- [88] **EROS-2** Collaboration, P. Tisserand *et al.*, “Limits on the Macho Content of the Galactic Halo from the EROS-2 Survey of the Magellanic Clouds,” *Astron. Astrophys.* **469** (2007) 387–404, [arXiv:astro-ph/0607207](#).
- [89] **Macho** Collaboration, R. Allsman *et al.*, “MACHO project limits on black hole dark matter in the 1-30 solar mass range,” *Astrophys. J. Lett.* **550** (2001) L169, [arXiv:astro-ph/0011506](#).
- [90] M. Oguri, J. M. Diego, N. Kaiser, P. L. Kelly, and T. Broadhurst, “Understanding caustic crossings in giant arcs: characteristic scales, event rates, and constraints on compact dark matter,” *Phys. Rev. D* **97** no. 2, (2018) 023518, [arXiv:1710.00148 \[astro-ph.CO\]](#).
- [91] **LIGO Scientific, Virgo** Collaboration, B. Abbott *et al.*, “Search for Substellar Mass Ultracompact Binaries in Advanced LIGO’s Second Observing Run,” *Phys. Rev. Lett.* **123** no. 16, (2019) 161102, [arXiv:1904.08976 \[astro-ph.CO\]](#).
- [92] S. Wang, Y.-F. Wang, Q.-G. Huang, and T. G. F. Li, “Constraints on the Primordial Black Hole Abundance from the First Advanced LIGO Observation Run Using the Stochastic Gravitational-Wave Background,” *Phys. Rev. Lett.* **120** no. 19, (2018) 191102, [arXiv:1610.08725 \[astro-ph.CO\]](#).
- [93] Z.-C. Chen and Q.-G. Huang, “Distinguishing Primordial Black Holes from Astrophysical Black Holes by Einstein Telescope and Cosmic Explorer,” *JCAP* **08** (2020) 039, [arXiv:1904.02396 \[astro-ph.CO\]](#).
- [94] V. Poulin, P. D. Serpico, F. Calore, S. Clesse, and K. Kohri, “CMB bounds on disk-accreting massive primordial black holes,” *Phys. Rev. D* **96** no. 8, (2017) 083524, [arXiv:1707.04206 \[astro-ph.CO\]](#).
- [95] Y. Ali-Haïmoud and M. Kamionkowski, “Cosmic microwave background limits on accreting primordial black holes,” *Phys. Rev. D* **95** no. 4, (2017) 043534, [arXiv:1612.05644 \[astro-ph.CO\]](#).
- [96] P. D. Serpico, V. Poulin, D. Inman, and K. Kohri, “Cosmic microwave background bounds on primordial black holes including dark matter halo accretion,” *Phys. Rev. Res.* **2** no. 2, (2020) 023204, [arXiv:2002.10771 \[astro-ph.CO\]](#).
- [97] Y. Ali-Haïmoud, E. D. Kovetz, and M. Kamionkowski, “Merger rate of primordial black-hole binaries,” *Phys. Rev. D* **96** no. 12, (2017) 123523, [arXiv:1709.06576 \[astro-ph.CO\]](#).
- [98] V. Vaskonen and H. Veermäe, “Lower bound on the primordial black hole merger rate,” *Phys. Rev. D* **101** no. 4, (2020) 043015, [arXiv:1908.09752 \[astro-ph.CO\]](#).

- [99] R.-G. Cai, S. Pi, and M. Sasaki, “Universal infrared scaling of gravitational wave background spectra,” [arXiv:1909.13728](#) [[astro-ph.CO](#)].
- [100] K. Inomata, M. Kawasaki, K. Mukaida, T. Terada, and T. T. Yanagida, “Gravitational Wave Production right after a Primordial Black Hole Evaporation,” *Phys. Rev. D* **101** no. 12, (2020) 123533, [arXiv:2003.10455](#) [[astro-ph.CO](#)].
- [101] P. Ajith *et al.*, “A Template bank for gravitational waveforms from coalescing binary black holes. I. Non-spinning binaries,” *Phys. Rev. D* **77** (2008) 104017, [arXiv:0710.2335](#) [[gr-qc](#)]. [Erratum: *Phys.Rev.D* 79, 129901 (2009)].
- [102] P. Ajith *et al.*, “Inspiral-merger-ringdown waveforms for black-hole binaries with non-precessing spins,” *Phys. Rev. Lett.* **106** (2011) 241101, [arXiv:0909.2867](#) [[gr-qc](#)].
- [103] P. Amaro-Seoane and Others, “Laser Interferometer Space Antenna,” *ArXiv e-prints* (Feb., 2017) , [arXiv:1702.00786](#) [[astro-ph.IM](#)].
- [104] **TianQin** Collaboration, J. Luo *et al.*, “TianQin: a space-borne gravitational wave detector,” *Class. Quant. Grav.* **33** no. 3, (2016) 035010, [arXiv:1512.02076](#) [[astro-ph.IM](#)].
- [105] J. Mei *et al.*, “The TianQin project: current progress on science and technology,” [arXiv:2008.10332](#) [[gr-qc](#)].
- [106] G. M. Harry, P. Fritschel, D. A. Shaddock, W. Folkner, and E. S. Phinney, “Laser interferometry for the big bang observer,” *Class. Quant. Grav.* **23** (2006) 4887–4894. [Erratum: *Class. Quant. Grav.* 23,7361(2006)].
- [107] N. Seto, S. Kawamura, and T. Nakamura, “Possibility of direct measurement of the acceleration of the universe using 0.1-Hz band laser interferometer gravitational wave antenna in space,” *Phys. Rev. Lett.* **87** (2001) 221103, [arXiv:astro-ph/0108011](#) [[astro-ph](#)].
- [108] L. Badurina *et al.*, “AION: An Atom Interferometer Observatory and Network,” *JCAP* **05** (2020) 011, [arXiv:1911.11755](#) [[astro-ph.CO](#)].
- [109] **AEDGE** Collaboration, Y. A. El-Neaj *et al.*, “AEDGE: Atomic Experiment for Dark Matter and Gravity Exploration in Space,” *EPJ Quant. Technol.* **7** (2020) 6, [arXiv:1908.00802](#) [[gr-qc](#)].
- [110] **LIGO Scientific** Collaboration, J. Aasi *et al.*, “Advanced LIGO,” *Class. Quant. Grav.* **32** (2015) 074001, [arXiv:1411.4547](#) [[gr-qc](#)].

- [111] **VIRGO** Collaboration, F. Acernese *et al.*, “Advanced Virgo: a second-generation interferometric gravitational wave detector,” *Class. Quant. Grav.* **32** no. 2, (2015) 024001, [arXiv:1408.3978 \[gr-qc\]](#).
- [112] **LIGO-India** Collaboration, B. Iyer *et al.*, “Proposal of the Consortium for Indian Initiative in Gravitational-wave Observations (IndIGO),” 2011. <https://dcc.ligo.org/LIGO-M1100296/public>.
- [113] C. Unnikrishnan, “IndIGO and LIGO-India: Scope and plans for gravitational wave research and precision metrology in India,” *Int. J. Mod. Phys. D* **22** (2013) 1341010, [arXiv:1510.06059 \[physics.ins-det\]](#).
- [114] **KAGRA** Collaboration, K. Somiya, “Detector configuration of KAGRA: The Japanese cryogenic gravitational-wave detector,” *Class. Quant. Grav.* **29** (2012) 124007, [arXiv:1111.7185 \[gr-qc\]](#).
- [115] **KAGRA** Collaboration, Y. Aso, Y. Michimura, K. Somiya, M. Ando, O. Miyakawa, T. Sekiguchi, D. Tatsumi, and H. Yamamoto, “Interferometer design of the KAGRA gravitational wave detector,” *Phys. Rev. D* **88** no. 4, (2013) 043007, [arXiv:1306.6747 \[gr-qc\]](#).
- [116] M. Punturo *et al.*, “The Einstein Telescope: A third-generation gravitational wave observatory,” *Class. Quant. Grav.* **27** (2010) 194002.
- [117] **LIGO Scientific** Collaboration, B. P. Abbott *et al.*, “Exploring the Sensitivity of Next Generation Gravitational Wave Detectors,” *Class. Quant. Grav.* **34** no. 4, (2017) 044001, [arXiv:1607.08697 \[astro-ph.IM\]](#).
- [118] **LIGO Scientific, Virgo** Collaboration, B. Abbott *et al.*, “Search for the isotropic stochastic background using data from Advanced LIGO’s second observing run,” *Phys. Rev. D* **100** no. 6, (2019) 061101, [arXiv:1903.02886 \[gr-qc\]](#).
- [119] C. J. Moore, R. H. Cole, and C. P. L. Berry, “Gravitational-wave sensitivity curves,” *Class. Quant. Grav.* **32** no. 1, (2015) 015014, [arXiv:1408.0740 \[gr-qc\]](#).
- [120] C. Périgois, C. Belczynski, T. Bulik, and T. Regimbau, “StarTrack predictions of the stochastic gravitational-wave background from compact binary mergers,” [arXiv:2008.04890 \[astro-ph.CO\]](#).
- [121] P. L. Bender, M. C. Begelman, and J. R. Gair, “Possible LISA follow-on mission scientific objectives,” *Class. Quant. Grav.* **30** (2013) 165017.

- [122] B. Canuel *et al.*, “ELGAR - a European Laboratory for Gravitation and Atom-interferometric Research,” [arXiv:1911.03701 \[physics.atom-ph\]](#).
- [123] **MAGIS** Collaboration, P. W. Graham, J. M. Hogan, M. A. Kasevich, S. Rajendran, and R. W. Romani, “Mid-band gravitational wave detection with precision atomic sensors,” [arXiv:1711.02225 \[astro-ph.IM\]](#).
- [124] **MAGIS-100** Collaboration, J. Coleman, “Matter-wave Atomic Gradiometer Interferometric Sensor (MAGIS-100) at Fermilab,” *PoS ICHEP2018* (2019) 021, [arXiv:1812.00482 \[physics.ins-det\]](#).
- [125] B. Canuel *et al.*, “Exploring gravity with the MIGA large scale atom interferometer,” *Sci. Rep.* **8** no. 1, (2018) 14064, [arXiv:1703.02490 \[physics.atom-ph\]](#).
- [126] W.-H. Ruan, Z.-K. Guo, R.-G. Cai, and Y.-Z. Zhang, “Taiji program: Gravitational-wave sources,” *Int. J. Mod. Phys. A* **35** no. 17, (2020) 2050075, [arXiv:1807.09495 \[gr-qc\]](#).
- [127] M.-S. Zhan *et al.*, “ZAIGA: Zhaoshan Long-baseline Atom Interferometer Gravitation Antenna,” *Int. J. Mod. Phys. D* **29** no. 04, (2019) 1940005, [arXiv:1903.09288 \[physics.atom-ph\]](#).
- [128] M. W. Choptuik, “Universality and scaling in gravitational collapse of a massless scalar field,” *Phys. Rev. Lett.* **70** (1993) 9–12.
- [129] J. C. Niemeyer and K. Jedamzik, “Near-critical gravitational collapse and the initial mass function of primordial black holes,” *Phys. Rev. Lett.* **80** (1998) 5481–5484, [arXiv:astro-ph/9709072](#).
- [130] A. M. Green and A. R. Liddle, “Critical collapse and the primordial black hole initial mass function,” *Phys. Rev. D* **60** (1999) 063509, [arXiv:astro-ph/9901268](#).
- [131] J. M. Bardeen, J. Bond, N. Kaiser, and A. Szalay, “The Statistics of Peaks of Gaussian Random Fields,” *Astrophys. J.* **304** (1986) 15–61.
- [132] M. Kawasaki and H. Nakatsuka, “Effect of nonlinearity between density and curvature perturbations on the primordial black hole formation,” *Phys. Rev. D* **99** no. 12, (2019) 123501, [arXiv:1903.02994 \[astro-ph.CO\]](#).
- [133] C. T. Byrnes, E. J. Copeland, and A. M. Green, “Primordial black holes as a tool for constraining non-Gaussianity,” *Phys. Rev. D* **86** (2012) 043512, [arXiv:1206.4188 \[astro-ph.CO\]](#).
- [134] S. Young and C. T. Byrnes, “Primordial black holes in non-Gaussian regimes,” *JCAP* **08** (2013) 052, [arXiv:1307.4995 \[astro-ph.CO\]](#).

- [135] R.-g. Cai, S. Pi, and M. Sasaki, “Gravitational Waves Induced by non-Gaussian Scalar Perturbations,” *Phys. Rev. Lett.* **122** no. 20, (2019) 201101, [arXiv:1810.11000 \[astro-ph.CO\]](#).
- [136] C. Yuan and Q.-G. Huang, “Gravitational waves induced by the local-type non-Gaussian curvature perturbations,” [arXiv:2007.10686 \[astro-ph.CO\]](#).
- [137] J. Garcia-Bellido, M. Peloso, and C. Unal, “Gravitational Wave signatures of inflationary models from Primordial Black Hole Dark Matter,” *JCAP* **09** (2017) 013, [arXiv:1707.02441 \[astro-ph.CO\]](#).
- [138] C. Unal, “Imprints of Primordial Non-Gaussianity on Gravitational Wave Spectrum,” *Phys. Rev. D* **99** no. 4, (2019) 041301, [arXiv:1811.09151 \[astro-ph.CO\]](#).
- [139] T. Nakama, J. Silk, and M. Kamionkowski, “Stochastic gravitational waves associated with the formation of primordial black holes,” *Phys. Rev. D* **95** no. 4, (2017) 043511, [arXiv:1612.06264 \[astro-ph.CO\]](#).
- [140] C. T. Byrnes, M. Hindmarsh, S. Young, and M. R. S. Hawkins, “Primordial black holes with an accurate QCD equation of state,” *JCAP* **08** (2018) 041, [arXiv:1801.06138 \[astro-ph.CO\]](#).
- [141] K. Jedamzik, “Primordial black hole formation during the QCD epoch,” *Phys. Rev. D* **55** (1997) 5871–5875, [arXiv:astro-ph/9605152](#).
- [142] F. Hajkarim and J. Schaffner-Bielich, “Thermal History of the Early Universe and Primordial Gravitational Waves from Induced Scalar Perturbations,” *Phys. Rev. D* **101** no. 4, (2020) 043522, [arXiv:1910.12357 \[hep-ph\]](#).
- [143] M. Takada, “Constraining PBH with microlensing,” in *Focus Week on Primordial Black Hole*, Kavli IPMU, U. of Tokyo. 12, 2019. <https://indico.ipmu.jp/event/301/timetable/#20191202.detailed>.
- [144] M. Hazumi *et al.*, “LiteBIRD: A Satellite for the Studies of B-Mode Polarization and Inflation from Cosmic Background Radiation Detection,” *J. Low Temp. Phys.* **194** no. 5-6, (2019) 443–452.
- [145] K. Abazajian *et al.*, “CMB-S4 Science Case, Reference Design, and Project Plan,” [arXiv:1907.04473 \[astro-ph.IM\]](#).
- [146] G. Franciolini, 9, 2020. private communication.